Ionic Liquid Based on α-Amino Acid Anion and N7,N9-Dimethylguaninium Cation ([dMG][AA]): Theoretical Study on the Structure and Electronic Properties

ARTICLE *in* THE JOURNAL OF PHYSICAL CHEMISTRY A · APRIL 2012

Impact Factor: 2.69 · DOI: 10.1021/jp211774y · Source: PubMed

3 AUTHORS, INCLUDING:

Mehdi Shakorian
Birjand University of Technology
30 PUBLICATIONS **101** CITATIONS
SEE PROFILE

Ahmad Bayat
Sharif University of Technology
9 PUBLICATIONS **36** CITATIONS
SEE PROFILE

THE JOURNAL OF PHYSICAL CHEMISTRY A

Article

pubs.acs.org/JPCA

Ionic Liquid Based on α-Amino Acid Anion and N7,N9-Dimethylguaninium Cation ([dMG][AA]): Theoretical Study on the Structure and Electronic Properties

Mehdi Shakourian-Fard, Alireza Fattahi,* and Ahmad Bayat

Department of Chemistry, Sharif University of Technology, P.O. Box 11365-9516, Tehran, Iran

Supporting Information

ABSTRACT: The interactions between five amino acid based anions ($[AA]^-$ (AA = Gly, Phe, His, Try, and Tyr)) and N7,N9-dimethylguaninium cation ($[dMG]^+$) have been investigated by the hybrid density functional theory method B3LYP together with the basis set 6-311++G(d,p). The calculated interaction energy was found to decrease in magnitude with increasing side-chain length in the amino acid anion. The interaction between the $[dMG]^+$ cation and $[AA]^-$ anion in the most stable configurations of ion pairs is a hydrogen bonding interaction. These hydrogen bonds (H bonds) were analyzed by the quantum theory of atoms in molecules (QTAIM) and natural bond orbital (NBO) analysis. Finally, several correlations between electron densities in bond critical points of hydrogen bonds and interaction energy as well as vibrational frequencies in the most stable configurations of ion pairs have been checked.

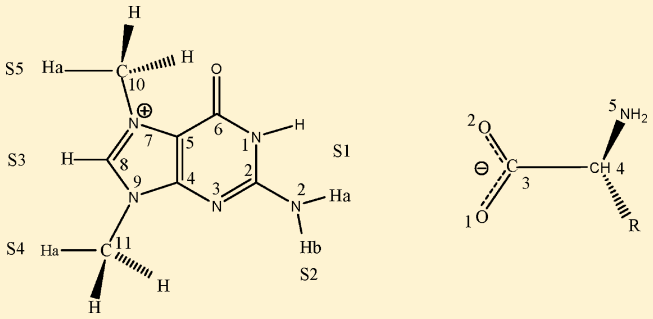

1. INTRODUCTION

Ionic liquids (ILs) are a class of novel compounds composed exclusively of organic cations and inorganic anions. Unlike ionic solids, in which the ions are relatively small and thus can pack closely to each other, the bulkiness of both the cation and anion prevents such packing, thereby lowering the lattice energy. Consequently, ionic liquids have been classified as ionic compounds that have melting points at temperatures of 100 °C or lower. In fact, many are liquid at or below room temperature, having melting points as low as −96 °C.[1] Recently, interest has tremendously increased in the room-temperature ionic liquids (RTILs),[2] which are ideal reaction solvents,[3] extraction solvents,[4] electrolyte materials,[5] and so on, due to their remarkable properties. To understand the properties of RTILs is, therefore, of fundamental importance not only for solvent alternatives but also for green chemistry.[6] However, commonly used RTILs are prepared with anions containing fluorine. Their utilization is usually associated with the release of HF and, consequently, jeopardizes the use of the liquids as "green" solvents. Obviously, the use of biologically relevant ions as precursors for preparing RTILs is a promising greener approach.[7]

Recently, much attention has been paid to the study of the various applications, the design, and the properties of new ILs. Many groups are still devoted to develop the new, functionalized RTILs. In particular, two classes of RTILs have recently been developed. The first is based on the nitrogen containing cations (e.g., imidazole and pyridine) and various inorganic anions;[8] the second is based on the imidazolium cation and various amino acid anions.[9] In terms of the new RTILs, ionic constituents and the size of IL seem to be critical. Early work indicated that the anionic constituents of ILs may have a greater influence on their physical and chemical properties.[10] However, recent studies have shown that the cationic constituent of ILs is important to the thermal stability of the IL.[11] They observed that the bulkier cations[11] and dicationic salts[12] rather than monocationic salts vastly improved the thermal stability of ILs. Thus, a bulkier cation seems to be another crucial factor to be considered for the design of new ILs.[13]

Guanine, one of the five nucleic acid bases, has the ability to store and transfer information through Watson−Crick base pairing. Moreover, guanine, in comparison to imidazole, has a larger volume and lower symmetry. Thus, the ionic liquid based on guaninium not only could improve its thermal stability but also has higher selectivity to nucleic acid, and so more favorable for some biological reactions.[14] Also, the N7,N9-dimethylguaninium cation with respect to the imidazolium cation has several suitable sites for interaction of anions via the hydrogen bond interaction. Therefore, it is interesting to investigate the most appropriate site for interaction of various anions with the N7,N9-dimethylguaninium cation and compare with the imidazolium cation in the ionic liquids. Herein, we report a series of ionic liquids whose cations and anions are derived from naturally occurring α-amino acids and N7,N9-dimethylated guanine that might be used as an IL. This kind of IL has the advantage of being green and can be introduced easily in synthetic processes.

Understanding the interactions at molecular level is important to predict the physicochemical properties and design of functional

Received: December 7, 2011
Revised: April 29, 2012

   dx.doi.org/10.1021/jp211774y | J. Phys. Chem. A XXXX, XXX, XXX−XXX

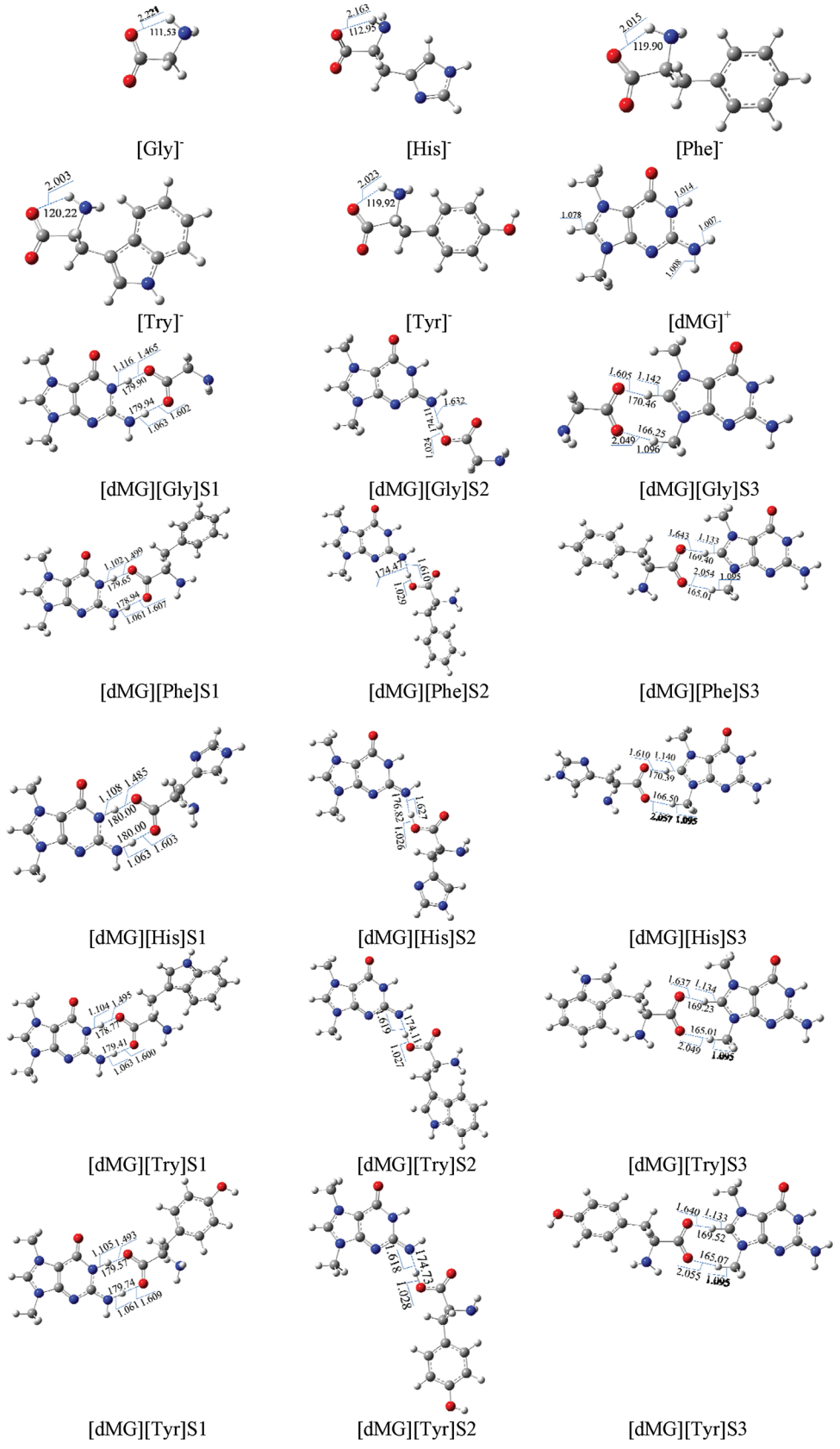

Figure 1. Optimized configurations of [dMG][AA] ion pairs. All bond lengths and angles are in angstroms and degrees, respectively.

amino acid ionic liquids (AAILs). Ohno et al.[9] first prepared the AAILs by coupling the 1-ethyl-3-methylimidazolium cation ($[emim]^+$) with 20 natural amino acid anions ($[AA]^-$). Kou et al.[15] reported a new generation of cations, which were directly derived from α-amino acids and their ester salts, and prepared novel natural ILs [AA]X (X = Cl^-, NO_3^-, BF_4^-, PF_6^-, ...)

dx.doi.org/10.1021/jp211774y | J. Phys. Chem. A XXXX, XXX, XXX−XXX

and [AAE]Y (Y = NO_3^-, BF_4^-, PF_6^-, Tf_2N^-, ...). Mou et al.[16] investigated the AAILs formed from $[emim]^+$ and the glycine anion $[Gly]^-$ and found that all the stable isomers were characterized by the intermolecular H bonds. Rong et al.[17] synthesized the glutamic acid based ILs, [Glu]X (X = BF_4^-, NO_3^-, Cl^-, PF_6^-, ...). Their research results indicated that the smaller value of binding energy between $[Glu]^+$ and acid anion leads to the lower melting point. Xing et al.[14] investigated the interactions of N7,N9-dimethylguaninium with different anions (F^-, Cl^-, Br^-, and BF_4^-) and explored the influence of anions on the properties of ion pairs.

In this work, we focus on the molecular interaction of several AAILs composed of the N7,N9-dimethylguaninium cation and amino acid anions ([dMG][AA] (AA = Gly, Phe, His, Try, and Tyr) ILs). Then, the effects of side-chain length of aromatic amino acid functional group on the nature of interaction have been investigated. Moreover, properties extracted from the quantum theory of atoms in molecules (QTAIM) and natural bond orbital analysis (NBO) were used to determine the nature and strength of intermolecular hydrogen bond interactions.

2. COMPUTATIONAL DETAILS

The structures of the [dMG][AA] (AA = Gly, Phe, His, Try, and Tyr) IL ion pairs and the corresponding monomers were optimized at B3LYP/6-311++G(d,p) level and single-point energy calculations have also been performed at the MP2/6-311++G(d,p) level using Spartan 06 software.[18] It is well understood that polarized and diffusive orbitals are needed to account for the H-bonded interactions. Vibrational frequencies were calculated to verify the stationary structure for all the structures. The interaction energies of the ion pairs are defined as follows:

$$\Delta E_{int} = E(\text{ion pair}) - E(\text{cation}) - E(\text{anion})$$

The zero-point vibrational energy corrections (ZPE) have been obtained within the harmonic approximation, and basis set superposition errors (BSSE) have been determined using the counterpoise method.[19] To examine the nature of interaction between the cation and the anions, natural bond orbital (NBO) analyses of the considered configurations have been performed by the B3LYP/6-311++G(d,p) method. The bond characteristics for the relevant configurations were also illustrated on the basis of quantum theory of atoms in molecules (QTAIM) analysis.[20] The topological properties were performed by using the AIM2000 package[21] with the wave functions generated from the B3LYP/6-311++G(d,p) results.

3. RESULTS AND DISCUSSION

3.1. Structures of Single Ions. In general, the overall energy of anion $[AA]^-$ (AA = Gly, Phe, His, Try, and Tyr) is mainly affected by the geometric distortion and the intramolecular hydrogen bonds. Here, as $[AA]^-$ is concerned, the intramolecular hydrogen bonds may play the important role in stabilizing the anion. To find the most stable conformer of $[AA]^-$ anions, different conformers of $[AA]^-$ on the potential energy surface at the relative energy range of 0−10 kcal/mol were determined using the Merck molecular force field (MMFF) provided in Spartan 06 software. Finally, the obtained conformers were optimized at the B3LYP/6-311++G(d,p) level. As seen in Figure 1, the most stable conforms of α-amino acid anions $[AA]^-$ (AA = Gly, Phe, His, Try, and Tyr) are stabilized by intramolecular H bond formed between oxygen atom of carbonyl and hydrogen atom of amino group. The N7,N9-dimethylguaninium cation ($[dMG]^+$) was also optimized directly at the B3LYP/6-311++G(d,p) level. The most stable geometry shows a planar structure with dihedral angles of 0.009°, 0.024°, 0.01°, and 0.035° for N2−C2−N3−C4, N2−C2−N1−C6, C10−N7−C5−C4, and C11−N9−C4−C5, respectively. Theses dihedral angles show that the amino and methyl groups are in-plane with the ring.

3.2. [dMG][AA] Ion Pairs. *3.2.1. Optimized Geometries.* In the case of [dMG][AA] ion pairs, the favorable sites of H bonds are located around the carbonyl oxygen atoms in $[AA]^-$ anion, and the N1−H, N2−Ha, N2−Hb, and C8−H bonds in $[dMG]^+$ cation (Scheme 1). Five regions of S1, S2, S3, S4, and S5 are favorable for the formation of intermolecular H bonds. The most stable configurations for interaction of $[AA]^-$ anions with the N1−H, N2−Ha, N2−Hb, and C8−H bonds in $[dMG]^+$ cation are shown in Figure 1. These configurations will be identified as [dMG][AA]S1 (interaction through N1−H and N2−Ha simultaneously), [dMG][AA]S2 (interaction through N2−Hb), and [dMG][AA]S3 (interaction through C8−H). As can be seen from the optimized structures of ion pairs, the interactions between the two fragments are characterized by both single and multiple H bonds that mainly formed between the electronegative O atoms of the $[AA]^-$ anion and the N−H, C−H bonds of the $[dMG]^+$ cation. The equilibrium distances between the proton and proton acceptor atom, referred to as the intrinsically preferred H bond length, along with the corresponding angle are shown in Figure 1. A hydrogen bond will be indicated if the H···X distance is less than the van der Waals H···X distance and the corresponding X−H···Y (X = O, N, or C, Y = O, N) angle is greater than 90°.[22]

As seen in Figure 1, in the configurations of [dMG][AA]S1 and [dMG][AA]S3 (AA = Gly, Phe, His, Try, and Tyr), the interactions occur between oxygen atoms of $[AA]^-$ anion and several sites of $[dMG]^+$ cation, including hydrogen atoms on nitrogen and carbon atoms (N1−H, N2−Ha, C8−H, and C11−Ha bonds). It is also seen that proton transfer does not occur in these structures, although the hydrogen atom on nitrogen (N2−Hb) in configurations of [dMG][AA]S2 has been taken away by the oxygen atom in anion. The corresponding ion pairs have turned to neutral pairs. Let us take the configuration [dMG][Gly]S2 for example; the N2−Hb distance has changed from 1.008 Å (in $[dMG]^+$ cation) to 1.632 Å in the ion pair, which is far beyond the length of a normal N−H covalent bond, whereas the O1−Hb bond length becomes a normal O−H covalent bond when the cation combines with the anion. This indicates that the proton Hb has transferred from cation to anion.

Scheme 1. Atomic Numbering of the Isolated $[dMG]^+$ Cation and $[AA]^-$ Anion[a]

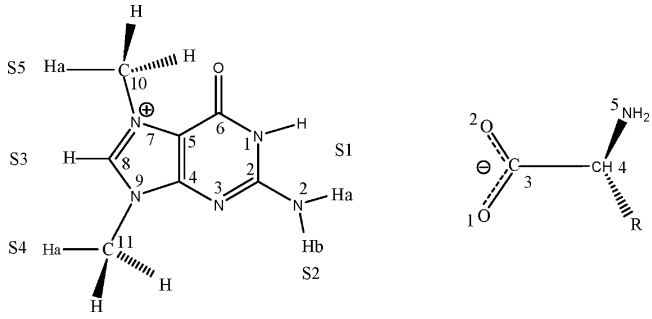

[a]S1−S5 denote the possible regions for interaction of anion $[AA]^-$ (AA = Gly, Phe, His, Try, and Tyr).

dx.doi.org/10.1021/jp211774y | J. Phys. Chem. A XXXX, XXX, XXX−XXX

Table 1. Absolute Energies (E_{SCF}, au), Calculated Interaction Energies (ΔE_{int}, kcal/mol) at 298 K, and the Relative Interaction Energies ($\Delta\Delta E_{int}$, kcal/mol) at the B3LYP/6-311++G(d,p) Level[a]

structure	E_{SCF}	ΔE_{int}	$\Delta\Delta E_{int}$	structure	E_{SCF}	ΔE_{int}	$\Delta\Delta E_{int}$
$[dMG]^+$	−621.545704			[dMG][Phe]S3	−1175.915098	−84.30	8.71
$[Gly]^-$	−283.904273			[dMG][His]S1	−1169.931675	−95.67	0
$[Phe]^-$	−554.229007			[dMG][His]S2	−1169.914807	−86.66	9.01
$[His]^-$	−548.228370			[dMG][His]S3	−1169.918688	−87.29	8.38
$[Try]^-$	−685.798438			[dMG][Try]S1	−1307.499029	−93.82	0
$[Tyr]^-$	−629.470598			[dMG][Try]S2	−1307.480022	−82.78	11.04
[dMG][Gly]S1	−905.610368	−99.42	0	[dMG][Try]S3	−1307.485606	−85.67	8.15
[dMG][Gly]S2	−905.592336	−88.67	10.75	[dMG][Tyr]S1	−1251.169559	−92.77	0
[dMG][Gly]S3	−905.596646	−89.11	10.31	[dMG][Tyr]S2	−1251.151124	−82.90	9.87
[dMG][Phe]S1	−1175.928277	−93.01	0	[dMG][Tyr]S3	−1251.156726	−84.16	8.61
[dMG][Phe]S2	−1175.909330	−82.70	10.31				

[a]Interaction energies are corrected with the basis set superposition error (BSSE).

Table 2. Absolute Energies (E_{SCF}, au), Calculated Interaction Energies (ΔE_{int}, kcal/mol) at 298 K, and the Relative Interaction Energies ($\Delta\Delta E_{int}$, kcal/mol) at the MP2/6-311++G(d,p)//B3LYP/6-311++G(d,p) Level[a]

structure	E_{SCF}	ΔE_{int}	$\Delta\Delta E_{int}$	structure	E_{SCF}	ΔE_{int}	$\Delta\Delta E_{int}$
$[dMG]^+$	−620.033122			[dMG][Phe]S3	−1173.032190	−87.58	9.06
$[Gly]^-$	−283.231629			[dMG][His]S1	−1167.099386	−99.12	0
$[Phe]^-$	−552.850812			[dMG][His]S2	−1167.082953	−90.07	9.04
$[His]^-$	−546.901996			[dMG][His]S3	−1167.087313	−90.41	8.70
$[Try]^-$	−684.091697			[dMG][Try]S1	−1304.286961	−97.55	0
$[Tyr]^-$	−627.932420			[dMG][Try]S2	−1304.269393	−86.58	10.97
[dMG][Gly]S1	−903.431014	−102.69	0	[dMG][Try]S3	−1304.274412	−89.13	8.42
[dMG][Gly]S2	−903.414533	−91.89	10.80	[dMG][Tyr]S1	−1248.125700	−96.23	0
[dMG][Gly]S3	−903.418051	−91.91	10.78	[dMG][Tyr]S2	−1248.108085	−86.11	10.12
[dMG][Phe]S1	−1173.044584	−96.64	0	[dMG][Tyr]S3	−1248.113674	−87.37	8.86
[dMG][Phe]S2	−1173.026711	−86.29	10.36				

[a]Interaction energies are corrected with the basis set superposition error (BSSE).

From Figure 1, it can be found that the structure of $[dMG]^+$ in [dMG][AA] ion pairs shows important changes in the bond lengths of N1−H, N2−Ha, N2−Hb, and C8−H in location of H bonds. For example, the bond length of N1−H changes from 1.014 Å in $[dMG]^+$ cation to 1.116 Å in the configuration [dMG][Gly]S1. On the other hand, in these configurations, $[AA]^-$ anion also remains in-plane with $[dMG]^+$ cation.

3.2.2. Interaction Energy of Ion Pairs. Table 1 lists the absolute energy of monomers, ion pairs and the interaction energies ΔE_{int} corrected by BSSE for [dMG][AA] ion pairs at the B3LYP/6-311++G(d,p) level. For the ion pairs, the interaction energies range from −99.42 to −82.70 kcal/mol. Generally, the H-bonded interaction energies of these ion pairs are comparable to conventional ionic liquids. In [emim]Cl, [emim]-$[BF_4]$, and [emim]$[PF_6]$ ion pairs, the interaction energies are reported to be about −90.98, −82.33, and −86.83 kcal/mol, respectively.[23] According to the interaction energy, it may be deduced that the melting point and viscosity of the [dMG][AA] ion pairs are comparable to that of [emim]Cl, [emim]$[BF_4]$, and [emim]$[PF_6]$ ion pairs. As shown in Table 1, the interaction energy values of [dMG][AA] (AA = Gly, Phe, His, Try, and Tyr) ion pairs follow the order [dMG][AA]S1 > [dMG][AA]S3 > [dMG][AA]S2. The [dMG][AA]S1 ion pairs are around 10−11 kcal mol^{-1} more stable than [dMG][AA]S2 and [dMG][AA]S3 ion pairs. For a closer look, interaction energies were calculated at MP2/6-311++G-(d,p)//B3LYP/6-311++G(d,p) level. Then, thermal corrections and BSSE corrections were included in the calculated interaction energies. As seen in Table 2, the order of relative interaction energies ($\Delta\Delta E_{int}$) at the MP2/6-311++G(d,p)//B3LYP/6-311++G(d,p) level is similar to the order obtained from B3LYP/6-311++G(d,p) level. MP2 results in agreement with DFT results confirm that [dMG][AA]S1 geometries have the most interaction energy. It seems that higher stability of [dMG][AA]S1 and [dMG][AA]S3 ion pairs is due to the presence of an additional hydrogen bonding. The large energy difference between [dMG][AA]S1 ion pairs and [dMG][AA]S2 and [dMG][AA]S3 ion pairs suggests that [dMG]-[AA]S1 ion pairs may be the expected structure from interaction of the $[dMG]^+$ cation and $[AA]^-$ anion. An increase of the side-chain length in the $[AA]^-$ anion produces a decrease of interaction energy. It can be due to the van der Waals force between the $[dMG]^+$ cation and the $[AA]^-$ anion. Thus, the anion moves far away from the $[dMG]^+$ and the H bonds of ion pairs become weaker. A similar effect has been also expected in conventional ionic liquids. The increase of anion size leads to weaker interaction energies and hydrogen bonds in ion pairs.

The variation of interaction energy for [dMG][AA]S1, [dMG]-[AA]S2, and [dMG][AA]S3 (AA = Gly, Phe, His, Try, and Tyr) ion pairs is presented in Figure 2. Considering the three types of ion pairs indicates that [dMG][Gly]S1, [dMG][Gly]S2, and [dMG][Gly]S3 ion pairs form the most stable configurations in each type of ion pairs. Also the stability of ion pairs decreases as the side-chain group of amino acid anion becomes larger. Despite the decrease of stability with the increase of side-chain length, in the interaction between a specific amino acid anion with $[dMG]^+$ cation, it has been observed that ion pairs formed in S1 region are more stable than those in S2 and S3 regions.

3.3. Properties of Ion Pairs. Chemists often ascribe the origin of X−H bond lengthening and the associated effects of a

dx.doi.org/10.1021/jp211774y | J. Phys. Chem. A XXXX, XXX, XXX−XXX

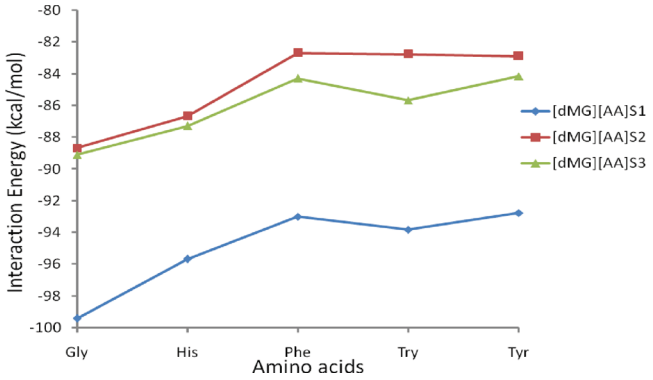

Figure 2. Interaction energy variation for [dMG][AA]S1, [dMG]-[AA]S2, and [dMG][AA]S3 (AA = Gly, Phe, His, Try, and Tyr) ion pairs.

proper H-bond to the result of the electrostatic interaction[24] or hyperconjugation interaction.[25] In the simplest explanation, electrostatic interaction causes X−H lengthening because the hydrogen acceptor atom pulls positive H closer to it and thus causes further polarization of the X−H bond, which not only increases the interaction but also increases the intensity of X−H stretching band in the IR.[13] The red shift of vibrational frequency occurs because of weakening of the associated X−H bond. In the explanation of the hyperconjugation interaction, the stabilization is due to the overlap of the vacant $\sigma^*_{X\text{-}H}$ antibonding orbital with the filled MO of the hydrogen acceptor atom (usually the lone pair).[25] Because the electron density transfers from the hydrogen acceptor atom to the σ^*_{X-H} antibonding orbital, the bond is weakened and lengthened. To better understand the nature of the binding between $[AA]^-$ anion and $[dMG]^+$ cation, the vibrational frequencies and NBO analysis are investigated.

3.3.1. IR Vibrations. Frequency analysis within the harmonic approximation has been performed for all optimized structures. The selected vibrational frequencies of the ion pairs and the isolated cation related to H-bonding are presented in Table 3. As presented in Table 3, the C/N−H···O hydrogen bonds all have frequency (stretching vibrations) changes in going from the isolated ions to the hydrogen-bonded structures. It is illustrated that these C/N−H bonds all have a red shift after formation of the

Table 3. Bond Lengths (r, Å) and C/O/N−H Vibrational Frequencies (cm^{-1}) for the Isolated Cation and Configurations [dMG][AA]S1, [dMG][AA]S2, and [dMG][AA]S3 (AA = Gly, Phe, His, Try, and Tyr)

structure	X−H	ν	$\Delta\nu^a$	r	Δr^b
$[dMG]^+$	N1−H	3568.17		1.014	
	N2−Ha	3601.27		1.006	
	N2−Hb	3601.27		1.008	
	C8−H	3273.60		1.077	
	C11−Ha	3165.62		1.088	
[dMG][Gly]S1	N1−H	1990.47	1577.7	1.116	0.102
	N2−Ha	2683.83	917.44	1.062	0.056
[dMG][Gly]S2	O1−Hb	2704.19	897.08	1.632	0.624
	N2−Ha	3537.35	63.92	1.016	0.009
[dMG][Gly]S3	C8−H	2340.56	933.04	1.142	0.064
	C11−Ha	2997.79	167.83	1.096	0.008
[dMG][Phe]S1	N1−H	2146.80	1421.37	1.102	0.088
	N2−Ha	2705.82	895.45	1.061	0.054
[dMG][Phe]S2	O1−Hb	2611.20	990.07	1.610	0.602
	N2−Ha	3538.76	62.51	1.016	0.009
[dMG][Phe]S3	C8−H	2465.30	808.30	1.133	0.055
	C11−Ha	3008.48	157.14	1.095	0.007
[dMG][His]S1	N1−H	2073.06	1495.11	1.108	0.094
	N2−Ha	2685.20	916.07	1.063	0.056
[dMG][His]S2	O1−Hb	2670.31	930.96	1.627	0.619
	N2−Ha	3541.08	60.19	1.015	0.008
[dMG][His]S3	C8−H	2366.17	907.43	1.140	0.062
	C11−Ha	2999.41	166.21	1.095	0.007
[dMG][Try]S1	N1−H	2120.68	1447.49	1.104	0.090
	N2−Ha	2682.30	918.97	1.063	0.056
[dMG][Try]S2	O1−Hb	2649.18	952.09	1.619	0.610
	N2−Ha	3536.95	64.32	1.016	0.009
[dMG][Try]S3	C8−H	2447.02	826.58	1.134	0.056
	C11−Ha	3006.19	159.43	1.095	0.007
[dMG][Tyr]S1	N1−H	2113.47	1454.7	1.105	0.091
	N2−Ha	2708.93	892.34	1.061	0.054
[dMG][Tyr]S2	O1−Hb	2640.09	961.18	1.618	0.609
	N2−Ha	3537.92	63.35	1.015	0.008
[dMG][Tyr]S3	C8−H	2457.28	816.32	1.133	0.055
	C11−Ha	3007.93	157.69	1.095	0.007

$^a\Delta\nu = \nu_{\text{ion pair}} - \nu_{\text{cation}}$. $^b\Delta r = r_{\text{ion pair}} - r_{\text{cation}}$.

dx.doi.org/10.1021/jp211774y | J. Phys. Chem. A XXXX, XXX, XXX−XXX

Table 4. Significant Natural Bond Orbital Interactions of [dMG][AA]S1, [dMG][AA]S2, and [dMG][AA]S3 (AA = Gly, Phe, His, Try, and Tyr) Ion Pairs and Their Second-Order Perturbation Stabilization Energies $E(2)$ (kcal/mol) Calculated at the B3LYP/6-311++G(d,p) Level

structure	charge transfer	$E(2)$	structure	charge transfer	$E(2)$
[dMG][Gly]S1	lp(O1) → σ*(N1−H)	74.57	[dMG][His]S3	lp(O1) → σ*(C8−H)	43.05
	lp(O2) → σ*(N2−Ha)	43.19		lp(O2) → σ*(C11−Ha)	7.82
[dMG][Gly]S2	lp(N2) → σ*(O1−Hb)	46.30	[dMG][Try]S1	lp(O1) → σ*(N1−H)	67.18
[dMG][Gly]S3	lp(O1) → σ*(C8−H)	44.38		lp(O2) → σ*(N2−Ha)	43.45
	lp(O2) → σ*(C11−Ha)	8.13	[dMG][Try]S2	lp(N2) → σ*(O1−Hb)	48.29
[dMG][Phe]S1	lp(O1) → σ*(N1−H)	66.06	[dMG][Try]S3	lp(O1) → σ*(C8−H)	39.05
	lp(O2) → σ*(N2−Ha)	42.36		lp(O2) → σ*(C11−Ha)	7.72
[dMG][Phe]S2	lp(N2) → σ*(O1−Hb)	73.11	[dMG][Tyr]S1	lp(O1) → σ*(N1−H)	67.90
[dMG][Phe]S3	lp(O1) → σ*(C8−H)	38.31		lp(O2) → σ*(N2−Ha)	42.16
	lp(O2) → σ*(C11−Ha)	7.53	[dMG][Tyr]S2	lp(N2) → σ*(O1−Hb)	71.02
[dMG][His]S1	lp(O1) → σ*(N1−H)	69.89	[dMG][Tyr]S3	lp(O1) → σ*(C8−H)	38.76
	lp(O2) → σ*(N2−Ha)	43.25		lp(O2) → σ*(C11−Ha)	7.53
[dMG][His]S2	lp(N2) → σ*(O1−Hb)	46.51			

Table 5. Selected Partial Charges from a NPA Analysis of [dMG][AA]S1, [dMG][AA]S2, and [dMG][AA]S3 (AA = Gly, Phe, His, Try, and Tyr) Ion Pairs at the B3LYP/6-311++G(d,p) Level

structure	N1	N1−H	N2	N2−Ha	N2−Hb	C8	C8−H	C11	C11−Ha	O1	O2	C3	N5
$[dMG]^+$	−0.609	0.424	−0.742	0.409	0.426	0.317	0.236	−0.355	0.219				
$[Gly]^-$										−0.791	−0.805	0.740	−0.878
$[Phe]^-$										−0.781	−0.787	0.756	−0.895
$[His]^-$										−0.780	−0.801	0.745	−0.891
$[Try]^-$										−0.784	−0.788	0.757	−0.898
$[Tyr]^-$										−0.781	−0.789	0.754	−0.897
[dMG][Gly]S1	−0.646	0.466	−0.756	0.446	0.391	0.276	0.218	−0.351	0.205	−0.762	−0.765	0.793	−0.838
[dMG][Gly]S2	−0.634	0.405	−0.781	0.353	0.510	0.274	0.215	−0.352	0.200	−0.728	−0.657	0.782	−0.833
[dMG][Gly]S3	−0.614	0.412	−0.773	0.391	0.411	0.326	0.307	−0.380	0.286	−0.806	−0.784	0.774	−0.841
[dMG][Phe]S1	−0.641	0.468	−0.750	0.448	0.392	0.275	0.218	−0.352	0.205	−0.758	−0.762	0.815	−0.867
[dMG][Phe]S2	−0.633	0.405	−0.782	0.354	0.510	0.276	0.216	−0.353	0.201	−0.724	−0.654	0.809	−0.864
[dMG][Phe]S3	−0.614	0.413	−0.773	0.391	0.412	0.328	0.304	−0.378	0.285	−0.801	−0.782	0.798	−0.872
[dMG][His]S1	−0.642	0.466	−0.751	0.447	0.391	0.272	0.217	−0.352	0.204	−0.753	−0.767	0.801	−0.852
[dMG][His]S2	−0.633	0.404	−0.779	0.350	0.509	0.275	0.215	−0.353	0.200	−0.721	−0.657	0.793	−0.847
[dMG][His]S3	−0.614	0.412	−0.774	0.391	0.411	0.326	0.305	−0.379	0.285	−0.798	−0.785	0.784	−0.857
[dMG][Try]S1	−0.641	0.468	−0.750	0.448	0.391	0.274	0.217	−0.352	0.204	−0.759	−0.763	0.817	−0.866
[dMG][Try]S2	−0.633	0.405	−0.781	0.354	0.510	0.275	0.215	−0.353	0.200	−0.725	−0.655	0.810	−0.863
[dMG][Try]S3	−0.615	0.413	−0.773	0.391	0.411	0.328	0.305	−0.378	0.285	−0.804	−0.783	0.799	−0.871
[dMG][Tyr]S1	−0.641	0.467	−0.750	0.448	0.391	0.271	0.218	−0.352	0.205	−0.756	−0.768	0.802	−0.854
[dMG][Tyr]S2	−0.633	0.405	−0.781	0.353	0.509	0.275	0.216	−0.353	0.201	−0.723	−0.659	0.795	−0.846
[dMG][Tyr]S3	−0.613	0.413	−0.773	0.391	0.412	0.327	0.305	−0.378	0.285	−0.800	−0.783	0.798	−0.873

ion pairs. The magnitudes of frequency changes for C/N−H bonds are generally in agreement with the trend of the magnitudes of C/N−H bond elongation.

The N1−H and N2−Ha bonds in configurations [dMG][AA]S1 have the largest elongation in comparison with C8−H and C11−Ha bonds in configurations [dMG][AA]S3 (Table 3); correspondingly, the N1−H and N2−Ha bonds have the largest value of frequency changes. These features indicate the formation of the true H bonds between the $[dMG]^+$ and $[AA]^-$ fragments. As seen from Table 3, the changes of bond lengths (Δr) and vaibrational frequencies ($\Delta\nu$) for N1−H and N2−Ha bonds in configurations [dMG][AA]S1 and C8−H and C11−Ha bonds in [dMG][AA]S3 decrease with increasing side-chain length in $[AA]^-$ anion. This result is in agreement with a decrease of interaction energy, when the side-chain length of $[AA]^-$ anion increases. Moreover, the disappearance of N2−Hb stretching vibration (3601.27 cm^{-1} in isolated cation) in configurations [dMG][AA]S2 and appearance of O1−Hb stretching vibration in these configurations show that the proton (Hb) has transferred from N2 atom to O1 in going from the isolated ions to configurations [dMG][AA]S2.

3.3.2. Charge Population and Bonding Analyses. NBOs provide the most accurate possible (natural Lewis structure) picture of the wave function ψ because all the orbital details are mathematically chosen to include the highest possible percentage of the electron density. A useful aspect of the NBO method is that it provides information about the interactions in both filled and virtual orbital spaces that facilitates the analysis of intra- and intermolecular interactions. A second-order perturbation theory analysis of the Fock matrix was carried out to evaluate the donor−acceptor interaction in the NBO basis. The interactions result in a loss of occupancy from the localized NBOs of the idealized Lewis structure into the empty non-Lewis orbitals.[25] In this analysis, a stabilization energy $E(2)$ related to the delocalization trend of electrons from donor to acceptor orbitals, was calculated via perturbation theory. If the stabilization energy $E(2)$ between a donor

dx.doi.org/10.1021/jp211774y | J. Phys. Chem. A XXXX, XXX, XXX−XXX

Table 6. Properties of the Electron Density (au) of Bond Critical Points (BCPs) for the Intermolecular Interactions in Configurations [dMG][AA]S1, [dMG][AA]S2, and [dMG][AA]S3 (AA = Gly, Phe, His, Try, and Tyr) Calculated at the B3LYP/6-311++G(d,p) Level

structure	BCP	P_c	λ_1	λ_2	λ_3	$\nabla^2\rho_c$
[dMG][Gly]S1	O1···H−N1	0.0854	−0.1925	−0.1874	0.5099	0.1300
	O2···Ha−N2	0.0605	−0.1168	−0.1125	0.3676	0.1384
[dMG][Gly]S2	N2···Hb−O1	0.0615	−0.1157	−0.1101	0.3267	0.1010
[dMG][Gly]S3	O1···H−C8	0.0629	−0.1194	−0.1150	0.3711	0.1367
	O2···Ha−C11	0.0218	−0.0265	−0.0261	0.1272	0.0745
[dMG][Phe]S1	O1···H−N1	0.0781	−0.1687	−0.1641	0.4681	0.1353
	O2···Ha−N2	0.0595	−0.1142	−0.1099	0.3622	0.1381
[dMG][Phe]S2	N2···Hb−O1	0.0652	−0.1255	−0.1195	0.3438	0.0987
[dMG][Phe]S3	O1···H−C8	0.0572	−0.1044	−0.1007	0.3401	0.1350
	O2···Ha−C11	0.0214	−0.0258	−0.0255	0.1253	0.0740
[dMG][His]S1	O1···H−N1	0.0814	−0.1789	−0.1743	0.4847	0.1315
	O2···Ha−N2	0.0603	−0.1162	−0.1118	0.3653	0.1373
[dMG][His]S2	N2···Hb−O1	0.0625	−0.1186	−0.1128	0.3311	0.0997
[dMG][His]S3	O1···H−C8	0.0621	−0.1172	−0.1130	0.3673	0.1371
	O2···Ha−C11	0.0215	−0.0260	−0.0255	0.1244	0.0729
[dMG][Try]S1	O1···H−N1	0.0791	−0.1717	−0.1671	0.4731	0.1343
	O2···Ha−N2	0.0605	−0.1170	−0.1127	0.3682	0.1385
[dMG][Try]S2	N2···Hb−O1	0.0637	−0.1215	−0.1157	0.3368	0.0997
[dMG][Try]S3	O1···H−C8	0.0581	−0.1067	−0.1029	0.3451	0.1355
	O2···Ha−C11	0.0216	−0.0262	−0.0259	0.1269	0.0748
[dMG][Tyr]S1	O1···H−N1	0.0796	−0.1732	−0.1685	0.4750	0.1333
	O2···Ha−N2	0.0593	−0.1135	−0.1092	0.3601	0.1374
[dMG][Tyr]S2	N2···Hb−O1	0.0638	−0.1219	−0.1160	0.3374	0.0994
[dMG][Tyr]S3	O1···H−C8	0.0577	−0.1055	−0.1017	0.3424	0.1352
	O2···Ha−C11	0.0214	−0.0258	−0.0254	0.1252	0.0738

bonding orbital and an acceptor orbital is large, then there is a strong interaction between them. For each donor orbital (i) and acceptor orbital (j), the stabilization energy $E(2)$ is associated with $i \rightarrow j$ delocalization, given by the following equation:

$$E(2) = \Delta E_{ij} = q_i \frac{F^2(i,j)}{\varepsilon_j - \varepsilon_i} \quad (1)$$

Where q_i is ith donor orbital occupancy; ε_j and ε_i are diagonal elements (orbital energies) and $F(i,j)$ is off diagonal elements associated with NBO Fock matrix.[26]

Table 4 lists the stabilization energies $E(2)$ of [dMG][AA]-S1, [dMG][AA]S2, and [dMG][AA]S3 (AA = Gly, Phe, His, Try, and Tyr) ion pairs estimated from the natural bond orbital (NBO) analysis at B3LYP/6-311++G(d,p) level. The large stabilizing effect is due to the strong orbital interactions between the antibonding orbital of proton donor $\sigma^*_{C/O/N-H}$ and the lone pairs of proton acceptor lp(O/N). The sum of stabilization energies for lp(O1) → σ^*(N1−H) and lp(O2) → σ^*(N2−Ha) interactions in the S1 region is much larger than that in S2 and S3 regions, which indicates these interactions contribute to the strong interaction between $[dMG]^+$ and $[AA]^-$.

Table 5 lists the selected natural population analyses (NPA) of [dMG][AA]S1, [dMG][AA]S2, and [dMG][AA]S3 ion pairs. It is clear that the charge distributions in the cation and anion of ion pairs are qualitatively comparable to those of the isolated ions. Different amino acid anions located around the $[dMG]^+$ cation have different effects on the charge distributions in the $[dMG]^+$ cation. It was found that the delocalization of negative charges varies with different side-chain structures of $[AA]^-$ anion. For example, the NPAs of O1, O2, and N5 atoms in $[Phe]^-$ anion are −0.781, −0.787, and −0.895e, respectively. These negative charges are relatively more delocalized than those of $[Gly]^-$ anion due to the functional group of benzene in $[Phe]^-$ anion.

Upon formation of hydrogen bonds, charge transfers occur from amino acid anions to $[dMG]^+$ cation. The extra electron density is distributed over the N1, N2, N1−H, and N2−Ha centers in [dMG][AA]S1. In configuration [dMG][AA]S3, the extra electron density is also dispersed over the C8, C8−H, C11, and C11−Ha centers, although the configuration [dMG][AA]S2 is resulted in the proton transfer (N2−Hb) from $[dMG]^+$ cation to O1 atom in $[AA]^-$ anion, when going from isolated $[dMG]^+$ and $[AA]^-$ to configuration [dMG]-[AA]S2. Thus, the electron density increases over the N2 center during the proton transfer. On the other hand, addition of $[dMG]^+$ cation to $[AA]^-$ anion causes the charges of $[AA]^-$ anion to be redistributed and the electrons transferred to the cation mainly from the O1, O2, C3, and N5 atoms (Table 5).

3.3.3. QTAIM Analysis. The bond properties between each pair of atoms were systematically analyzed using quantum theory of atoms in molecules (QTAIM),[20] which is based on the topological analysis of electron density (ρ_c) and its Laplacian ($\nabla^2\rho_c$) at the bond critical points (BCPs). The Laplacian $\nabla^2\rho_c$ at the BCP is the sum of the three curvatures of the density at the critical point, the two perpendicular to the bond path, λ_1 and λ_2, being negative (by convention, $\lambda_1 > \lambda_2$) whereas the third, λ_3, lying along the bond path, is positive. The negative curvatures measure the extent to which the density is concentrated along the bond path and the positive curvature measures the extent to which it is depleted in the region of the interatomic surface and concentrated in the individual atomic basins. In covalent bonding the two negative curvatures are dominant and $\nabla^2\rho_c < 0$; in contrast, in closed-shell bonding, for example, ionic, hydrogen bonding, or van der Waals

dx.doi.org/10.1021/jp211774y | J. Phys. Chem. A XXXX, XXX, XXX−XXX

interactions, the interaction is characterized by a depletion of density in the region of contact of the two atoms and $\nabla^2\rho_c > 0$. ρ_c is used to describe the strength of a bond, a stronger bond associated with a larger ρ_c value. In general, ρ_c is greater than 0.20 au in shared (covalent) bonding and less than 0.10 au in a closed-shell interaction.[27] From the values of electron density listed in Table 6, it can be concluded that the interactions between the $[dMG]^+$ cation and $[AA]^-$ anion, which are marked by the dotted line, are all closed-shell systems (H bonding interaction).

The values of $\nabla^2\rho_c$ are all positive. These values are within the commonly accepted values for normal H-bonding (0.02−0.139 au),[28] thus indicating the typical closed-shell interactions of these complexes. As seen in Table 6, the values of electron density for hydrogen bonding interactions in configurations [dMG][AA]S1 decrease with the increase of side-chain length in $[AA]^-$ anion. This decrease in electron density in BCPs can be due to decrease of interaction energy with the increase of side-chain length of $[AA]^-$ anion.

For hydrogen bonds, there is a correlation between the interaction energy and topological parameters at the BCPs.[29] Here, the existence of such a correlation has been checked for configurations [dMG][AA]S1. Figure 3 presents the linear correlation between the interaction energy and sum of electron densities in two intermolecular BCPs in configurations [dMG][AA]S1 (R^2 = 0.967).

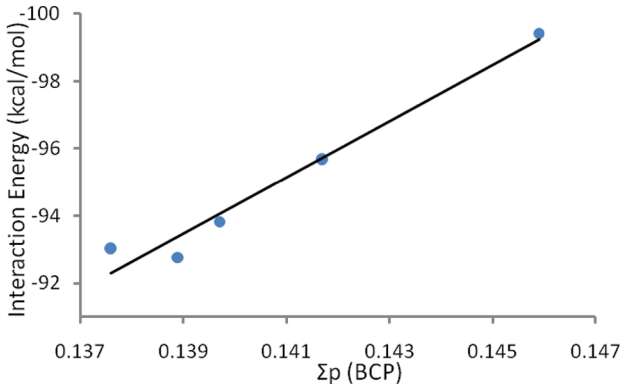

Figure 3. Correlation between interaction energy and sum of electron densities at BCPs of two hydrogen bonds in configurations [dMG][AA]S1.

Vibrational frequencies of N1−H and N2−Ha bonds as a function of electron density at BCPs of O1···H−N1 and O2···Ha−N2 hydrogen bonds in configurations [dMG][AA]S1 are shown in Figure 4a,b. As seen in Figure 4, the vibrational frequencies of N1−H and N2−Ha bonds decrease with the increase of electron density of H-bonding between cation and anion. For example, the value of electron density for O1···H−N1 hydrogen bond in [dMG][Gly]S1 is about 0.0854, which is significantly larger than that for a O1···H−N1 hydrogen bond in the other configurations of [dMG][AA]S1 (AA = Phe, His, Try, and Tyr). The largest value of electron density for the O1···H−N1 hydrogen bond in [dMG][Gly]S1 is also in agreement with the least vibrational frequency for the N1−H bond (1990.47 cm^{-1}). In the configurations of [dMG][AA]S1, the O1···H−N1 hydrogen bonds are stronger than O2···Ha−N2 hydrogen bonds (see ρ_c values in Table 6). This is in agreement with higher vibrational frequency changes of N1−H bonds compared with those of N2−Ha bonds.

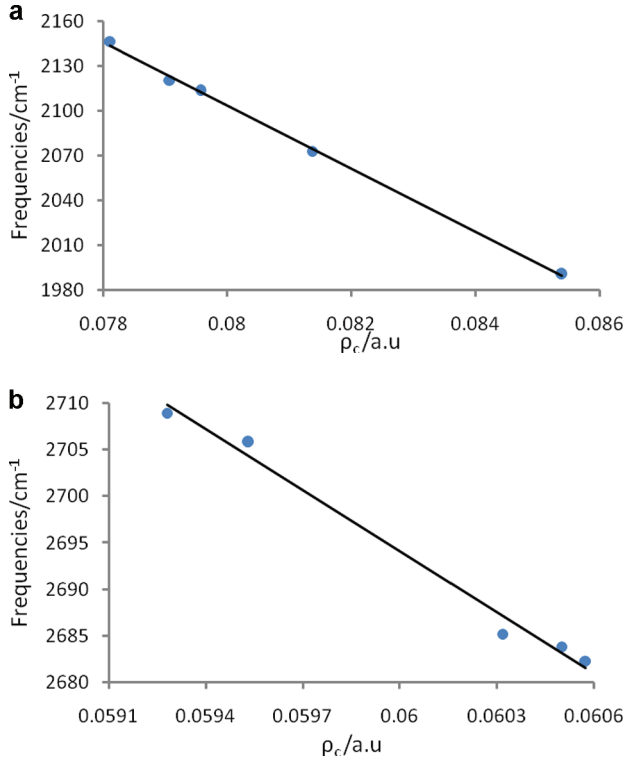

Figure 4. Vibrational frequencies of N1−H (a) and N2−Ha (b) bonds as a function of electron density at BCPs of O1···H−N1and O2···Ha-N2 hydrogen bonds in configurations [dMG][AA]S1, respectively (R^2 = 0.998 and 0.988, respectively).

4. CONCLUSION

In this study, a systematic study on the structure, electronic properties, and molecular interaction in amino acid ionic liquids composed of N7,N9-dimethylguaninium cation ($[dMG]^+$) and α-amino acid anions $[AA]^-$ (AA = Gly, Phe, His, Try, and Tyr) have been investigated. Among all studied amino acid anions and $[dMG]^+$ cation, the $[Gly]^-$ anion was found to form the most stable ion pair in the S1 region (interaction through N1−H and N2−Ha simultaneously). Also the stability of ion pairs in this region (S1) decreases as the side-chain group of the amino acid anion becomes larger. The nature of intermolecular H-bonds in ion pairs is investigated by the quantum theory of atoms in molecules (QTAIM) and natural bond orbital (NBO) analyses. From the QTAIM results, it can be concluded that the interactions between the $[dMG]^+$ cation and $[AA]^-$ anion are all closed-shell systems.

The results of NBO analysis show that the sum of stabilization energies ($E(2)$) for interactions in S1 region is much larger than that in S2 and S3 regions, which indicates these interactions contribute to the strong interaction between $[dMG]^+$ cation and $[AA]^-$ anion.

It is also seen that there is a good correlation between vibrational frequencies of H donors (N1−H and N2−Ha bonds) and the values of electron densities in bond critical points of two intermolecular H-bonds in the most stable configurations in S1 region ([dMG][AA]S1 (AA = Gly, Phe, His, Try, and Tyr)). It was indicated that with the increase of electron density in BCPs of H-bonds, the vibrational frequencies of N1−H and N2−Ha bonds decrease.

The results of QTAIM show that there is a linear correlation between the interaction energy and sum of electron densities in

dx.doi.org/10.1021/jp211774y | J. Phys. Chem. A XXXX, XXX, XXX−XXX

two intermolecular BCPs in the most stable configurations ([dMG][AA]S1 ion pairs). These conclusions will be helpful for detailed understanding of these AAILs and will contribute to the design and synthesis of AAILs in a "task specific" way.

■ ASSOCIATED CONTENT

Supporting Information

Cartesian coordinates of all optimized structures used in this work. This material is available free of charge via the Internet at http://pubs.acs.org.

■ AUTHOR INFORMATION

Corresponding Author

*E-mail: fattahi@sharif.edu.

Notes

The authors declare no competing financial interest.

■ ACKNOWLEDGMENTS

Support from Sharif University of technology is gratefully acknowledged.

■ REFERENCES

(1) Turner, E. A.; Pye, C. C.; Singer, R. D. *J. Phys. Chem. A* **2003**, *107*, 2277.
(2) Wilkes, J. S.; Zaworotko, M. J. *J. Chem. Soc., Chem. Commun* **1992**, *13*, 965.
(3) Welton, T. *Chem. Rev.* **1999**, *99*, 2071.
(4) Visser, A. E.; Swatloski, R. P.; Reichert, W. M.; Mayton, R.; Sheff, S.; Ierbicki, A.; Davis, J. H., Jr.; Rogers, R. D. *Chem. Commun* **2001**, *1*, 135.
(5) Yoshizawa, M.; Narita, A.; Ohno, H. *Aust. J. Chem.* **2004**, *57*, 139.
(6) Holbrey, J. D.; Seddon, K. R. *Clean Products Processes* **1999**, *1*, 223.
(7) Wu, Y.; Zhang, T. *J. Phys. Chem. A* **2009**, *113*, 12995.
(8) (a) Singh, R. P.; Verma, R. D.; Meshri, D. T.; Shreeve, J. M. *Angew.Chem., Int. Ed* **2006**, *45*, 3584. (b) Dymek, C. J.; Grossie, D. A.; Fratini, A. V.; Adams, W. W. *J. Mol. Struct.* **1989**, *213*, 25.
(9) Fukumoto, K.; Yoshizawa, M.; Ohno, H. *J. Am. Chem. Soc.* **2005**, *127*, 2398.
(10) Forsyth, S. A.; Pringle, J. M.; MacFarlane, D. R. *Aust. J. Chem.* **2004**, *57*, 113.
(11) Anderson, J. L.; Armstrong, D. W. *Anal. Chem.* **2003**, *75*, 4851.
(12) Anderson, J. L.; Ding, R.; Ellern, A.; Armstrong, D. W. *J. Am. Chem. Soc.* **2005**, *127*, 593.
(13) Xing, D.; Bu, Y.; Tan, X. *J. Phys. Chem. A* **2008**, *112*, 106.
(14) Xing, D.; Tan, X.; Zhang, C.; Bu, Y. *J. Mol. Struct.: THEOCHEM* **2010**, *939*, 82.
(15) Tao, G. H.; He, L.; Sun, N.; Kou, Y. *Chem. Commun* **2005**, *28*, 3562.
(16) Mou, Z. X.; Li, P.; Wang, W.; Shi, J.; Song, R. *J. Phys. Chem. B* **2008**, *112*, 5088.
(17) Rong, H.; Li, W.; Chen, Z. Y.; Wu, X. M. *J. Phys. Chem. B* **2008**, *112*, 1451.
(18) *Spartan '06V102'*; Wavefunction, Inc.: Irvine, CA.
(19) Boys, S. F.; Bernardi, F. *Mol. Phys.* **1970**, *19*, 553.
(20) Bader, R. F. W. *Atom in Molecules: A Quantum Theory*; Oxford University Press: New York, 1990.
(21) Bader, R. F. W. *AIM2000 program package*, Ver. 2.0; McMaster University: Hamilton, Ontario, Canada, 2002.
(22) Bondi, A. *J. Phys. Chem.* **1964**, *68*, 441.
(23) Dong, K.; Zhang, S. J.; Wang, D.; Yao, X. Q. *J. Phys. Chem. A* **2006**, *110*, 9775.
(24) Dykstra, C. E. *Acc. Chem. Res.* **1988**, *21*, 355.
(25) Reed, A.; Curtiss, L. A.; Weinhold, F. *Chem. Rev.* **1988**, *88*, 899.
(26) Bader, R. F. W. *Chem. Rev.* **1991**, *91*, 893.
(27) Gao, H.; Zhang, Y.; Wang, H. J.; Liu, J.; Chen, J. *J. Phys. Chem. A* **2010**, *114*, 10243.
(28) Mohajeri, A.; Ashrafi, A. *J. Phys. Chem. A* **2011**, *115*, 6589.
(29) Mohajeri, A.; Fadaei, F. *J. Phys. Chem. A* **2008**, *112*, 281.